Fachtagung "Experimentelle Strömungsmechanik"
5. – 7. September 2017, Karlsruhe

Untersuchungen zur Fluid-Struktur-Interaktion einer luftgestützten Halbkugelmembran unter turbulenter Zuströmung

Studies on the Fluid-Structure Interaction of a Pressurized Membranous Hemisphere in Turbulent Flow

Jens Nikolas Wood, Michael Breuer
Helmut-Schmidt-Universität
Professur für Strömungsmechanik
Holstenhofweg 85
22043 Hamburg
E-Mail: wood@hsu-hh.de, breuer@hsu-hh.de

Fluid-Struktur-Interaktion, Membranstruktur, turbulente Strömung, Particle-Image-Velocimetry, Digitale Bildkorrelation
Fluid-structure interaction, membranous structures, turbulent flow, particle-image-velocimetry, digital-image correlation

Abstract

In modern civil engineering the application of light-weight membranous structures is growing due to their high grade of spatial flexibility. This raises important issues in order to ensure the safe operation of this type of building such as the response of the flexible structure to wind loads. The present study contributes to this challanging topic by investigating the fluid-structure interaction (FSI) of a flexible thin-walled membranous hemispherical structure exposed to turbulent flow. Three Reynolds numbers (50,000, 75,000 and 100,000) are chosen to examine the interaction between the flow field and the pressurized membrane in a subsonic wind tunnel. As a reference the flow field around a rigid hemisphere is measured under identical conditions. The experiments are carried out by utilizing particle-image-velocimetry (PIV) for the flow field and high-speed digital-image correlation (DIC) measurements for the deformation of the unsteady structure excitations. Furthermore, constant-temperature anemometry (CTA) is applied to determine the velocity spectrum at predefined points close to the surface of the membranous structure. An analysis of the comprehensive data sets for the fluid flow and the displacements of the structure leads to the characterization of the behavior of the flexible structure under changing flow conditions.

Introduction

Pre-stressed membranous structures such as tents or air-supported buildings are gaining more attention in modern urban planning. Due to their high grade of spatial and temporal utilization they offer a wide range of applications spanning from locally fixed entertainment centers to temporal emergency shelters depicted in Fig. 1. Using membranes as major structural elements evokes important design issues. A complex phenomenon is the response of the flexible structure to wind loads especially in the case of turbulent boundary layers having a dramatic impact on the stability of such structures. The present experimental study focuses on a thin-walled air-inflated membranous hemisphere in turbulent flow. The model is put into a wind tunnel and exposed to an artificially generated turbulent boundary layer as described

Karlsruhe, Germany, ISBN 978-3-9816764-3-3

(a) Entertainment Center (Astana)[1] (b) uLites emergency shelter project[2]

Fig. 1: Various applications of pre-stressed membranous tents and inflatable structures.

by Wood and Breuer (2015, 2016) and Wood et al. (2016). Comprehensive particle-image-velocimetry (PIV) measurements of the flow field and digital-image correlation (DIC) measurements are carried out to characterize the fluid-structure interaction between the excited structure and the turbulent flow field. The results are compared with the flow around a rigid model of identical dimensions at Reynolds numbers of Re = 50,000, 75,000 and 100,000. Furthermore, constant-temperature anemometry is used to determine the velocity spectra at specific points close to the surface of the hemisphere. These are brought into correlation with the oscillation of the structure to find characteristic frequencies that are used to explain the complex interaction process.

Experimental Setup

The experimental setup is depicted in Figure 2. The model is immersed into a turbulent boundary layer. Specially designed turbulence generators are used to obtain the desired mean velocity profiles and turbulence intensities. The velocity profiles are measured at a distance $x/D = -1.5$ (with D = 150 mm the diameter of the hemisphere) with a special CTA boundary layer probe without placing the model inside the test section. All three Reynolds numbers show a comparable distribution and are in good agreement with the 1/7 power law. The Reynolds number is based on the free-stream velocity U_∞ and the diameter D of the hemisphere. Properties of air are assumed under standard atmospheric conditions (μ_{air} = 18.72 x 10^{-6} kg/(ms) and ρ_{air} = 1.225 kg/m³).

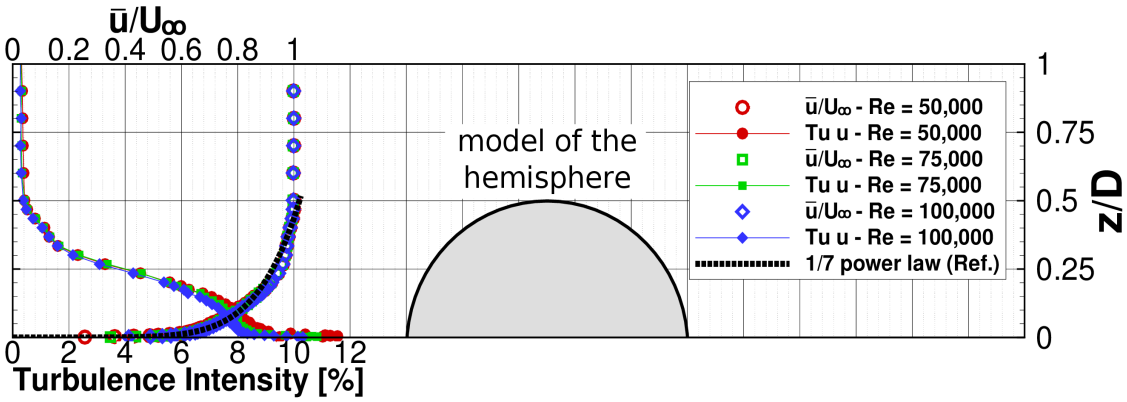

Fig. 2: Velocity profiles and turblence intensities of the turbulent boudary layer in the wind tunnel.

[1] http://ge.archello.com/en/project/khan-shatyr-entertainment-center/image-8

[2] http://www.cimne.com/websasp/ulites/

The model of the flexible hemisphere is made of silicone with an average thickness of the wall $\bar{t} = 0.16$ mm consisting of a total mass of 12.44 g. A detailed description of the material properties is given in Wood and Breuer (2016).

Table 1: Properties of the turbulent boundary layer at the Reynolds numbers investigated.

Reynolds number	**50,000**	**75,000**	**100,000**
free-stream velocity U_∞	5.14 m/s	7.64 m/s	10.24 m/s
max. turbulence level in boundary layer	11.5 %	10.8 %	10.1 %

Measurement Equipment used for Fluid-Structure Interaction

To capture the coupled problem of the flexible membrane under wind loads, serveral measurement techniques are used. The flow field is measured by a high-spatial resolution mono-PIV setup using a CCD camera with 29MP at a maximum sampling rate of 1.67 fps. The resolution is capable to resolve small-scale turbulence at larger camera distances. This offers the advantage of a large evaluation area without chaning the camera position too often. Each measurement contains 1500 double-images. The post-processing is carried out on a Nyquist grid with a spot dimension set to 24 x 24 pixel which translates to a cell size of 1.52 mm x 1.52 mm. DEHS is used as seeding medium and is atomized at the receiver of the wind tunnel.
The three-dimensional structure deformations are measured by a high-speed camera system in a steroscopic setup based on a digital-image correlation algorithm. The frame rate is set to 250 fps at an image resolution of 1503 x 996 pixels. Each data set contains 5611 images.
Additionally, a standard hot-film probe is applied to determine the velocity spectra at specific monitoring points close to the surface of the flexible hemisphere at a rate of 2000 Hz. Furthermore, a dynamic pressure transducer is utilized to measure the gauge pressure inside the model which has to be brought up to stabilize the membrane against the wind loads. For each Reynolds number a different pressurization is appied (Δp_{FSI1} = 19 Pa (Re = 50,000), Δp_{FSI2} = 34 Pa (Re = 75,000) and Δp_{FSI3} = 43 Pa (Re = 100,000)) to maintain the hemispherical shape.

Results

Unsteady flow field in the wake region

Figure 3 depicts an arbitrary snapshot of the instantaneous flow field in the wake of the flexible hemisphere at Re = 75,000. A highly turbulent flow field with a prominent recirculation containing numerous vortical structures is visible. Kelvin-Helmholtz instabilities are observable at the apex of the hemisphere arising from the separating shear layer.

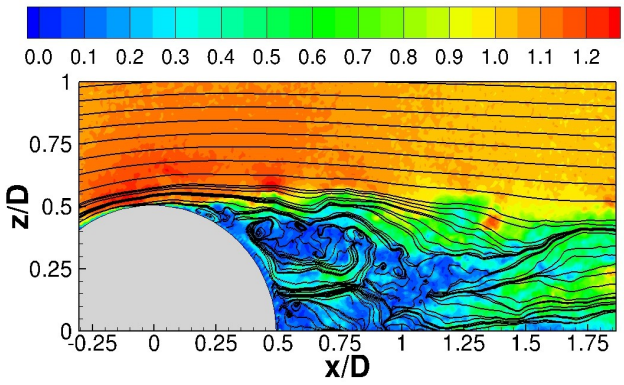

Fig. 3: Unsteady flow field (velocity magnitude) in the wake including streamlines (Re = 75,000).

Time-averaged flow field

The time-averaged flow fields are used to identify differences in the flow characteristics between the rigid and the flexible hemisphere at each Re number separately. Figure 4 depicts the time-averaged streamwise velocity superimposed by streamlines.

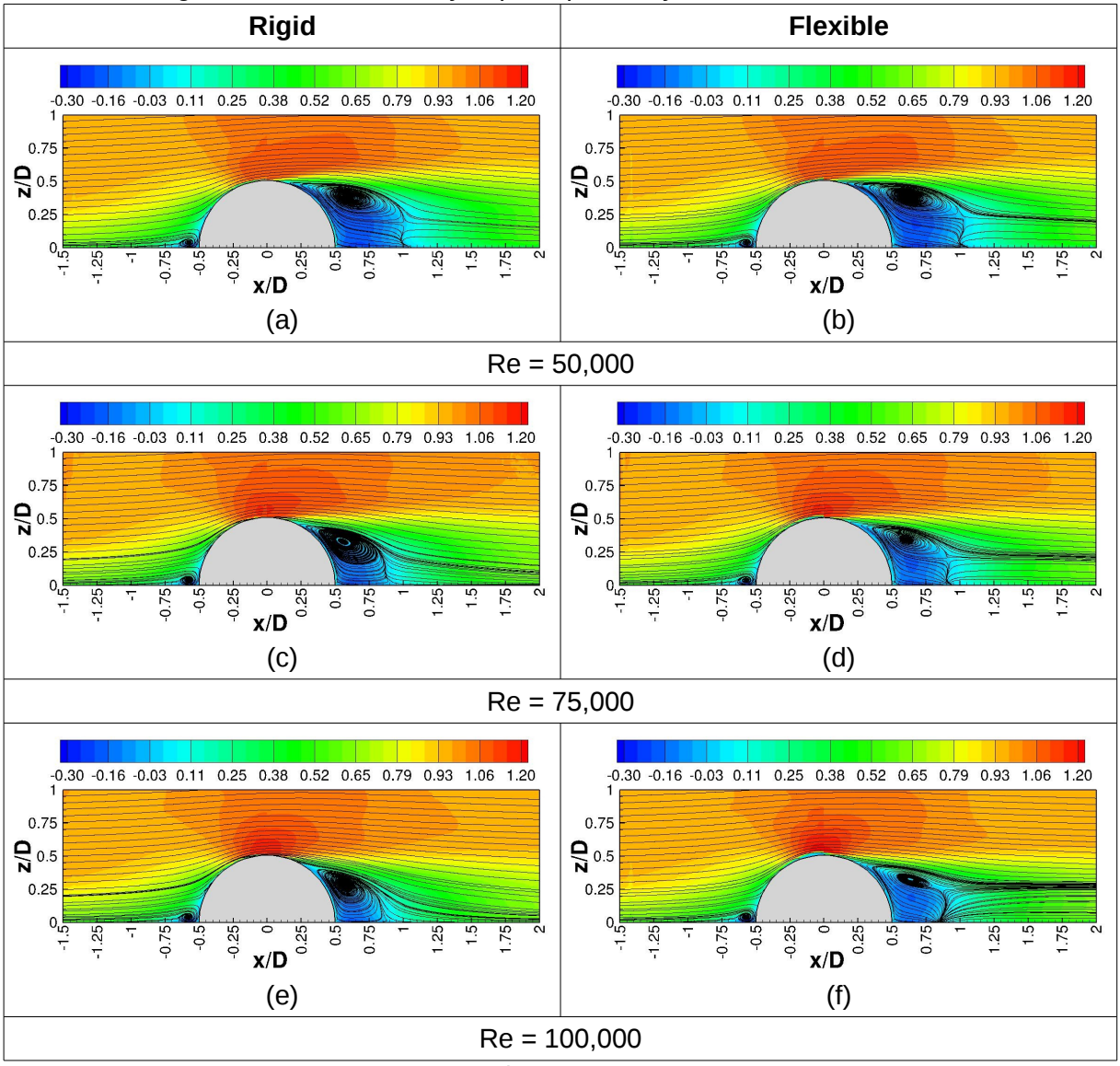

Fig. 4: Time-averaged streamwise velocity $\bar{u}/U_\infty$ superimposed by streamlines.

The flow field at Re = 50,000 in Figs. 4(a) and (b) exhibits only marginal differences due to the moderate free-stream velocity leading to very small structure deformations with little impact on the flow character. This changes with increasing Reynolds number. At Re = 75,000 (Figs. 4(c) and (d)) the shape of the recirculation area between the rigid and the flexible case changes visibly. Even more significant deviations in the flow field can be seen at Re = 100,000, since the structure deformations are largest compared to the lower Re numbers. Here the shape of the recirculation is remarkably different in case of the flexible hemisphere visible by the development of the streamlines. In the rigid case the dividing streamline is approaching the ground shorty after it passes the recirculation area, while in the flexible case it moves almost parallel to the ground. Interestingly, there are no significant changes in the upstream flow field. Thus, this flow area seems to be independent of the investigated Re number range.

Profile plots are used to quantify the discrepancies between the solid and the membranous model. All obtainable first and second-order moments are given in Fig. 5 for Re = 100,000. As mentioned above, the upstream region and the front side of the hemisphere exhibit no visible differences. Increasing changes in the profiles are detectable starting at about *x/D = 0* connected to the separation of the shear layer at the apex of the hemisphere. Major deviations between the rigid and the flexible hemisphere occur in the recirculation area especially obserable for the wall-normal velocity component. Furthermore, the sharp peak in the profile of the streamwise normal Reynolds stress in Fig. 5(c) at *x/D = 0* close to the surface of the flexible hemisphere indicates a separation further upstream compared to the rigid case. Generally, the Reynolds stresses in the wake of the flexible model are significantly lower leading to the hypothesis that the oscillations of the flexible structure have a damping effect on the flow field fuctuations.

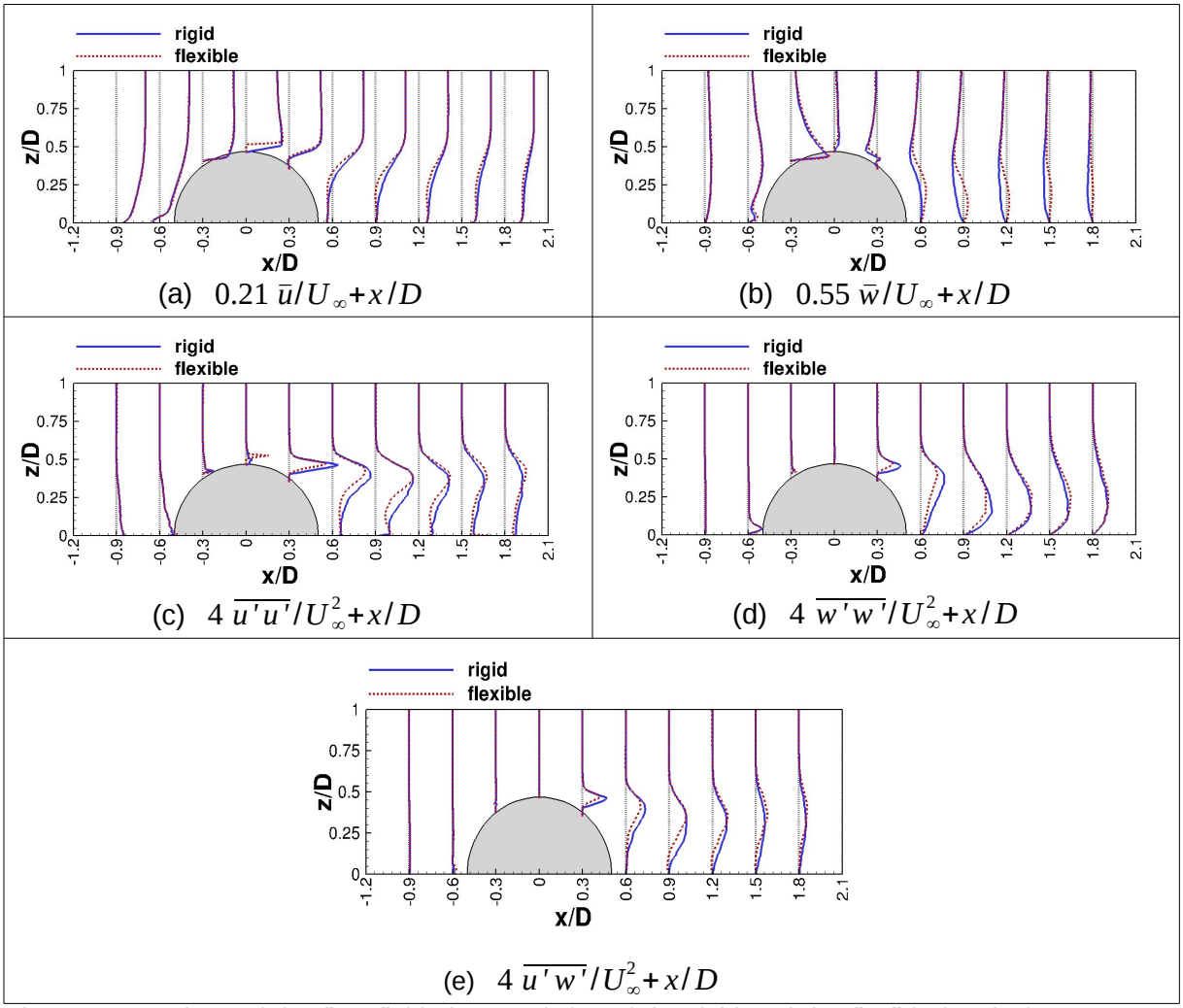

Fig. 5: Comparison of the flow field characteristics of the rigid and the flexible hemisphere at Re = 100,000.

Unsteady deformations

The series of graphs in Fig. 6 depicts the temporal development of the unsteady deformations caused by the turbulent flow acting on the outer surface of the deformable membrane at Re = 100,000. Total displacements $\Delta r = \sqrt{\Delta x^2 + \Delta y^2 + \Delta z^2}$ are used for the color mapping showing complex deformation patterns traveling across the flexible surface. The two dark spots in the correlation area are caused by reflections of the applied high-power lighting source. This leads to an overexposure of the image and no correlations are detectable.

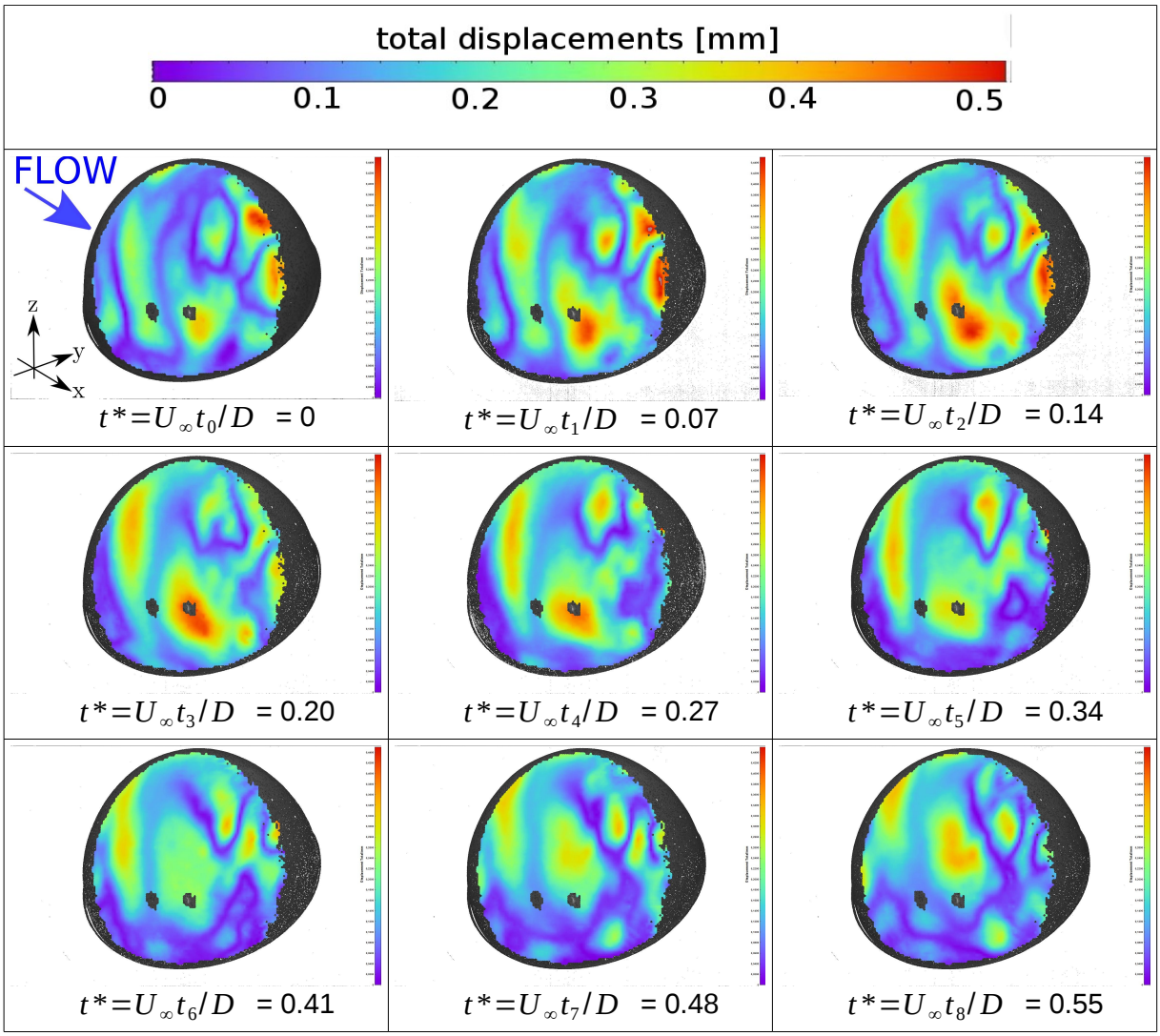

Fig. 6: Unsteady deformation patterns of the flexible hemisphere at Re = 100,000; view from the back-side of the model.

Structure deformation characteristics

To further analyze the experimental data of the three-dimentional deformations a 2D-profile on the lee side of the flexible hemisphere is extracted schematically shown in Fig. 7 (black dashed line). The chosen line element is in the symmetry plane of the hemisphere. In order to characterize the behavior of the structure oscillations, standard deviations of the displacements Δx and Δz are used. Figure 7(a) displays the standard deviation S_x/D of the streamwise displacements. With increasing Reynolds number the region of maximal fluctuations gradually narrows and is shifted towards the ground floor. The largest magnitudes of fluctuations $S_x/D = 1.75 \times 10^{-3}$ are present at $x/D = 0.4$ for Re = 100,000. The wall-normal displacements depicted in Fig. 7(b) indicate the opposite: Here the magnitude of the movement of the flexible structure decreases when approaching locations close to the ground. In this region the vertical oscillations of the structure are very small compared to the streamwise direction. The maximum fluctuations ($S_z/D = 1.65 \times 10^{-3}$) of the wall-normal component occur at $x/D = 0.12$ for Re = 100,000. These observations have their origin in strong excitations induced by the roll-up of vortices in the shear layer developing shortly after the separation line due to the Kelvin-Helmholtz instability.

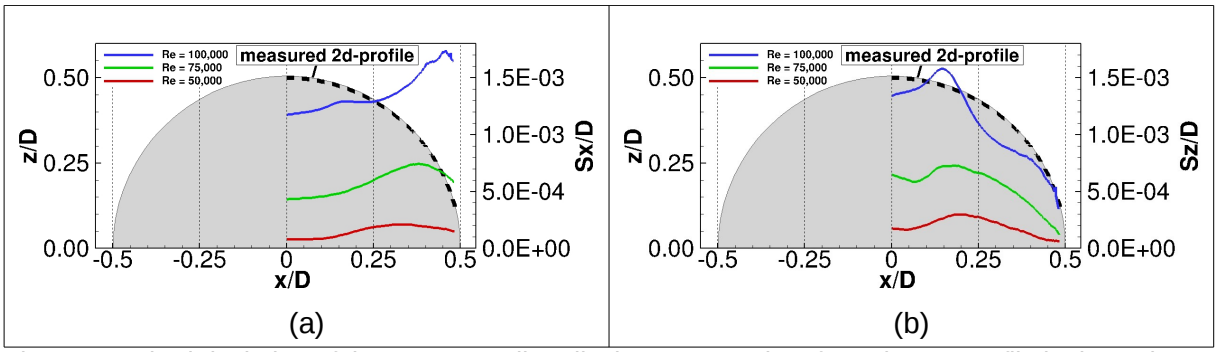

Fig. 7: Standard deviation of the corresponding displacements taken from the 2D-profile in the wake.

Fluid-structure interaction investigations

To correlate the structure deformation measurements with the fluid measurements, additional experiments using a standard hot-film CTA probe are carried out. As mentioned above, the PIV measurements revealed a significant difference between the Reynolds stresses in the wake of the rigid and the flexible case. This is especially eminent close to the surface of the hemisphere and strongest at Re = 100,000. A link between the structural movement and the fluid field is achieved by comparing the spectra of the oscillating structure based on the DIC measurements with the velocity spectra taken from the CTA measurements close to a monitoring point as depicted in Fig. 8. Due to different setup requirements and data recording length, the measurements have to be carried out independently.

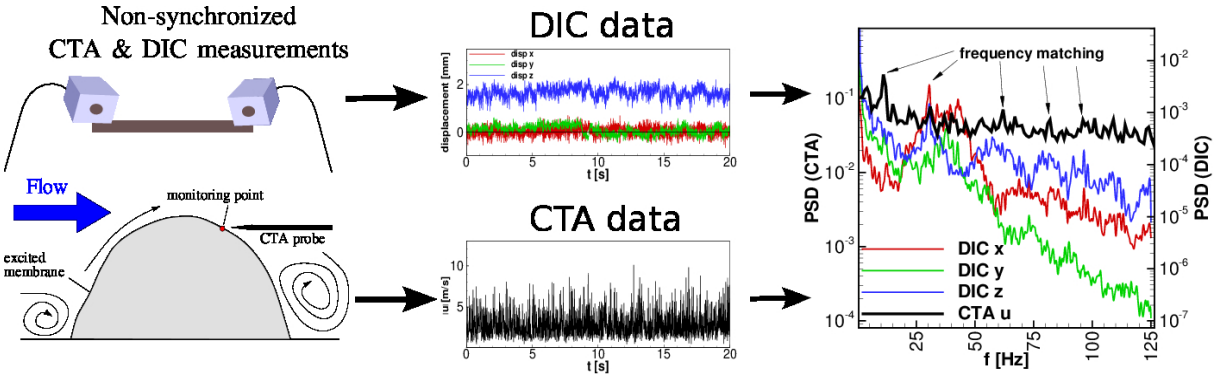

Fig. 8: Schematic principle of combined CTA and DIC measurements at a single monitoring point used for the comparison of characteristic frequency spectra.

The examined spectra at a single monitoring point in the wake (located at θ = 75°; further details about coordinate definition in Wood and Breuer (2016)) exhibit a complex distribution of frequencies (see Fig. 9). A typical vortex shedding frequencies of about 11 Hz is detectable that corresponds to a Strouhal number of St = $D\,f/U_\infty$ = 0.165. Furthermore, serveral natural frequencies f_n^i of the excited flexible hemisphere are visbile in both spectra. These eigenfrequencies were previously determined by a standardized dynamic response test outside the wind tunnel. As a result it is possible to link various frequencies from each measurement tool to identify characteristics of the underlying fluid-structure interaction phenomena. In the ongoing research gaps in the frequency spectra that cannot be matched to their physical origin yet are further analyzed. Especially, a large amplitude at about 30Hz which is found in the structure and the fluid domain with comparable strength remains to be clarified.

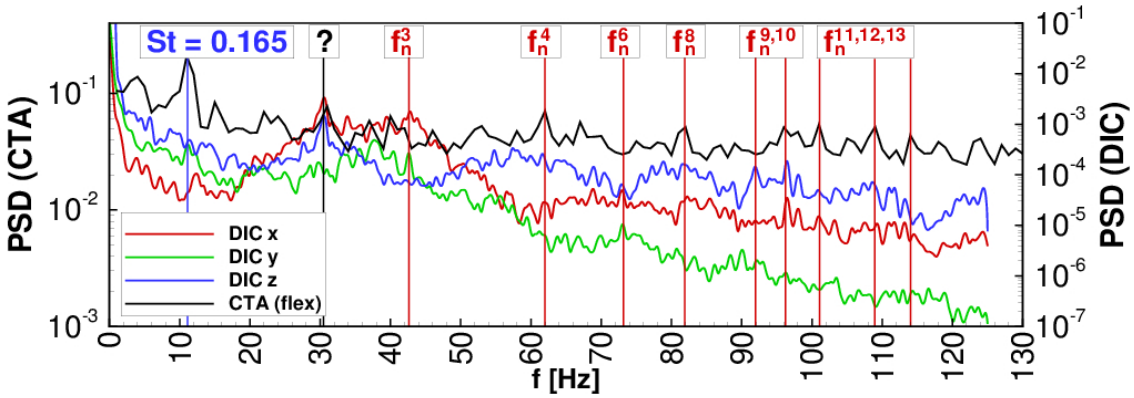

Fig. 9: Characteristic frequency spectra at a specific monitoring point located at θ = 75° in the wake.

Conclusions

Experimental measurements of the fluid-structure interaction of a wall-mounted air-inflated membranous hemisphere in turbulent flow were carried out at Re = 50,000, 75,000 and 100,000. Furthermore, the flow around a rigid hemisphere was studied under identical conditions and used as reference. Different measurement techniques were applied to determine the complex interaction between the oscillating membrane and the surrounding turbulent flow field. High-spatial resolution particle-image-velocimetry was used to measure the two-dimensional flow field in the symmetry plane of each hemisphere leading to the time-averaged first and second-order moments. A high-speed camera system recorded the structural deformations which were processed by digital-image correlation to receive the three-dimensional displacements. The time-averaged flow fields between the rigid and the flexible case differ with increasing Re number clearly visible in the streamlines. Especially the Reynolds stresses in the wake regime are significantly lower in case of the flexible hemisphere leading to an overall altered flow behavior. In a next step the structure oscillations were evaluated along a line in the wake that matches the PIV measurement plane. The standard deviation of the displacements in streamwise and wall-normal direction are augmented with increasing Re due to the amplified deflections that occur at higher wind loads. Frequency spectra of the membrane excitations were evaluated at specific points along the line to characterize the structural behavior in turbulent flow. Based on the PIV and DIC data, it is assumed that the oscillating structure dampens the velocity fluctuations in the wake region. To validate the interaction between the fluid field and the flexible structure, CTA was applied to record the velocity spectra close to the surface at points from the corresponding DIC measurement. It was possible to match characteristic frequencies, such as vortex shedding or natural frequency response of the structure. Nevertheless, there are still open issues which have to be analyzed in detail to fully describe the complex fluid-structure interaction phenomena of the present case.

References

Wood, J. N., Breuer, M., 2015: "Towards FSI: LDA-Investigations of the Flow past a Hemisphere in an Artificially Generated Turbulent Boundary Layer", 23. Fachtagung “Lasermethoden in der Strömungsmesstechnik”, 8.-10. Sept. 2015, Dresden, pp. 30-1-30-8

Wood, J. N., De Nayer, G., Schmidt, S., Breuer, M., 2016: "Experimental Investigation and Large-Eddy Simulation of the Turbulent Flow past a Smooth and Rigid Hemisphere", Flow, Turbulence and Combustion, vol. 97, pp. 97-119

Wood, J. N., Breuer, M., 2016: "Complementary Experimental-Numerical Investigation of the Flow past a Rigid and a Flexible Hemisphere in Turbulent Flow: Part 1: Experimental Measurements", 24. Fachtagung “Experimentelle Strömungsmechanik”, 6.-8. Sept. 2016, Cottbus, pp. 44-1-44-8

Wood, J. N., Breuer, M., De Nayer, G., 2017: "Studies on the Instantaneous Fluid-Structure Interaction of an Air-Inflated Flexible Membrane in Turbulent Flow – Part I: Experimental Investigations", (in preparation)